# The Effects of Molecular Weight and Temperature on the Kinetic Friction of Silicone Rubbers

Katherine Vorvolakos and Manoj K. Chaudhury*

*Department of Chemical Engineering, Lehigh University, Bethlehem, Pennsylvania 18015*

*Received December 23, 2002. In Final Form: May 14, 2003*

The frictional stresses of poly(dimethylsiloxane) elastomers of various molecular weights were measured against a supported monolayer of hexadecylsiloxane and a thin film of polystyrene as a function of sliding velocity and temperature. On both surfaces, friction decreases with molecular weight, but increases with sliding velocity, reaches a maximum, and thereafter it decreases or displays a plateau. While the velocity corresponding to the maximum shear stress is nearly independent of the molecular weight of the polymer, it differs between the two substrates. These results are consistent with the models proposed earlier by Schallamach as well as by Chernyak and Leonov, according to which the detachment force per load-bearing chain increases with velocity while the number of chains supporting the total frictional load decreases with velocity and molecular weight. From the temperature-dependent studies, the activation energy of friction on both surfaces is estimated to be ~25 kJ/mol, which is larger than the activation energy of viscous flow of silicone fluids, but compares well with the values obtained from recent studies of melt dynamics.

## Introduction

Frictional properties of soft elastomers are of importance in a variety of settings, such as the shear resistance of viscoelastic adhesives,[1,2] biofouling control,[3] road traction of automotive tires,[4] durability of windshield wipers,[5,6] and slippery prosthetic devices,[7–10] to name a few. There is, however, an incomplete understanding of the molecular level parameters that control the frictional behavior of elastomeric surfaces. Early experiments[11–13] on commercial natural rubber products were performed for the sole purpose of tabulating properties for consumers. Such tabulation persisted until the early 1950s, when Roth et al.[14] and Thirion[15] began experiments with the purpose of understanding the physics of rubber sliding. Quantitative physical analysis began with the observation that the classic Coulombic laws, obeyed consistently at interfaces between rigid bodies, fail at the interface between a rigid solid and a rubber.

Papenhuyzen[16] as well as Roth et al.[14] observed that the friction force of commercial rubbers on steel increases monotonically with velocity. Beyond a certain velocity, however, sliding becomes unstable and the rubber sample "chatters", or exhibits stick–slip sliding. Thirion,[15] on the other hand, observed that the friction increases with normal load, which was interpreted by Schallamach[17] to be due to the increase of contact area resulting from the deformation of rubber asperities. Similar suggestions were made by Bowden and Tabor.[18] Assuming the asperities to be hemispheres in Hertzian contact with smooth glass, Schallamach predicted that friction force would increase in a power law manner, with an exponent of 2/3. Indeed, this prediction was verified over a limited range of normal load. However, Schallamach did not immediately address a potentially fascinating finding that the friction force increases with modulus. If friction force depends on contact area, it is clear that a softer material would have a greater contact area for any load, therefore exhibiting higher friction, contrary to several experimental observations. Schallamach's hypothesis is therefore incomplete. He moved on to examine the effects of velocity and temperature[19] on rubber friction. As temperature increases, frictional force decreases. Alternatively, at a given temperature, the friction force increases with sliding velocity. Schallamach showed that the velocity- and temperature-dependent behavior of rubber friction follows Eyring's[20] theory of reaction rates. When this theory is applied to explain friction, interfacial sliding is presumed to proceed by the formation and breakage of molecular bonds at the interface in separate, thermally activated events.

While Schallamach focused on the molecular processes at the interface, Greenwood and Tabor[21] as well as Bueche and Flom[22] pointed out that the energy of sliding a soft

---

* To whom correspondence should be addressed at mkc4@lehigh.edu.

(1) Newby, B. Z.; Chaudhury, M. K.; Brown, H. R. *Science* **1995**, *269* (5229), 1407.

(2) Newby, B-m.; Chaudhury, M. K. *Langmuir* **1998**, *14*, 4865.

(3) Vorvolakos, K.; Chaudhury, M. K. In *Microstructure and Microtribology of Polymer Surfaces*; ACS Symposium Series 741; American Chemical Society: Washington, DC, 2000; pp 83–90.

(4) Aggarwal, S. L.; Fabris, H. J.; Hargis, I. G.; Livigni, R. A. *Polym. Prepr. (Am. Chem. Soc., Div. Polym. Chem.)* **1985**, 26 (2), 3.

(5) Theodore, A. N.; Samus, M. A.; Killgoar, P. C. *Ind. Eng. Chem. Res.* **1992**, *31* (12), 2759.

(6) Extrand, C. W.; Gent, A. N.; Kaang, S. Y. *Rubber Chem. Technol.* **1991**, *64* (1), 108–117.

(7) Dong, H.; Bell, T.; Blawert, C.; Mordike, B. L. *J. Mater. Sci. Lett.* **2000**, *19* (13), 1147.

(8) Wang, J.; Stroup, E.; Wang, X.; Andrade J. D. *Proc. SPIE-Int. Soc. Opt. Eng. Int. Conf. Thin Film Phys. Appl.* **1991**, Pt. 2 835.

(9) Murayama, T.; McMillin, C. R. *J. Appl. Polym. Sci.* **1983**, *28* (6), 1871.

(10) Nusbaum, H. J.; Rose, R. M.; Paul, I. L.; Crugnola, A. M.; Radin, E. L. *J. Appl. Polym. Sci.* **1979**, *23* (3), 777.

(11) Ariano, R. *India Rubber J.* **1930**, *79* (2), 56–58.

(12) Derieux, J. B. *J. Elisha Mitchell Sci. Soc.* **1934**, *50*, 53–55.

(13) Dawson, T. R. *Rubber: Physical and Chemical Properties*; Dawson, T. R., Porritt, B. D., Eds.; The Research Association of British Rubber Manufacturers: Croydon, U.K., 1935; pp 381–386.

(14) Roth, F. L.; Driscoll, R. L.; Holt, W. L. *J. Res. Natl. Bur. Stand.* **1942**, *28* (4), 439–462.

(15) Thirion, P. *Rev. Gen. Caoutch.* **1946**, *23* (5), 101–106.

(16) Papenhuyzen *Ingenieur* **1938**, *53*, V75.

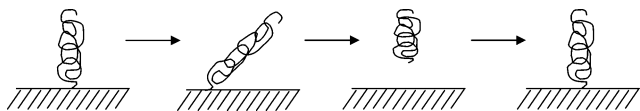(17) Schallamach, A. *Proc. Phys. Soc., London, Sect. B* **1952**, *65*, 657–661.

(18) Bowden, F. P.; Tabor, D. *The Friction and Lubrication of Solids*; Clarendon Press: Oxford, 1950.

(19) Schallamach, A. *Proc. Phys. Soc. London, Sect. B* **1952**, *66*, 386–392.

(20) Eyring, H. *J. Chem. Phys.* **1936**, *4*, 283.

(21) Greenwood, J. A.; Tabor, D. *Proc. Phys. Soc., London* **1958**, *71*, 989–1001.

(22) Bueche, A. M.; Flom, D. G. *Wear* **1959**, *2*, 168.

**Figure 1.** The classic depiction of a polymer chain in contact with a laterally moving countersurface. The chain stretches, detaches, relaxes, and reattaches to the surface to repeat the cycle.



**Figure 2.** The left figure qualitatively depicts the behavior of the areal density of contact points and the force per adsorption point as a function of velocity. The former decreases, while the latter increases up to a value limited by the interaction strength between the polymer chain and the countersurface. The product of these two quantities yields the shear stress, which increases and subsequently decreases, depicted on the right.
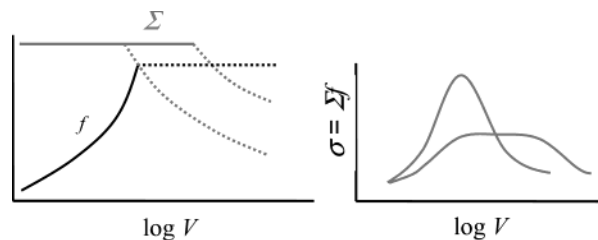
viscoelastic material over a rigid substrate is not spent entirely in breaking molecular contacts at the interface, but at least partially on deforming the soft material.

The notion that friction might be a combination of surface and bulk effects prompted Grosch[23] to perform the most systematic study in the field to date. He measured the effects of velocity, temperature, and surface roughness, while noting the synthetic makeup of the elastomers. Grosch observed that the rubber friction increases non-linearly with velocity, much like the shear thinning behavior of high viscous polymers. Above a certain critical velocity, the friction force exhibits a stick–slip behavior with the maximum friction in each pulse decreasing with velocity. Furthermore, at each sliding velocity, friction decreases with increasing temperature. All these temperature- and velocity-dependent frictional data can be assembled in a single master curve with the help of the well-known superposition principle of Williams, Landel, and Ferry.[24]

For rubber sliding on optically smooth glass, Grosch noted that velocity corresponding to maximum friction and the frequency corresponding to maximum viscoelastic loss form a ratio that is nearly constant (~7 nm) for various materials. He rationalized this observation by asserting that the interfacial relaxation processes responsible for friction are related to the segmental relaxation of the polymer chain. The length scale of 7 nm represents a molecular length, presumably the characteristic length by which the molecular jumps occur during the sliding process. For rough surfaces, the relevant length scale was found to be the characteristic spacing between surface asperities. Grosch's general observations of the dependence of friction on velocity and temperature were also supported by Extrand et al.,[6] who examined the more practical geometry of sharp rubber edges against rigid surfaces. Extrand et al. noted that the coefficient of friction depends strongly on the local load and the results are dependent on the surface preparation, i.e., chlorination of natural rubber.

Prompted by Grosch's observations, Schallamach[25] refined his model of interfacial friction, since a prediction of a monotonic dependence of friction on velocity was clearly insufficient. He maintained that unlubricated sliding on smooth surfaces is essentially adhesive in nature, mediated by separate bonding and debonding events between the rubber and the rigid surface, depicted in Figure 1.

Schallamach's[25] explanation of Grosch's[23] observations was based on the rate-dependent molecular debonding model of Frenkel[24] and Eyring.[20] In this model, the probability of debonding a polymer chain from a surface is a product of two functions, the first being the frequency factor that increases exponentially with the applied force and the second being the number of load-bearing chains that decreases with velocity. The solution of the kinetic rate equation resulting from such considerations leads to

an expression for the debonding force that increases with velocity, while the number of the load-bearing polymer chains ($\Sigma$) decreases (Figure 2). The net effect is that the total interfacial stress at first increases with velocity, reaches a maximum, and thereafter decreases with velocity.

Recently, Chernyak and Leonov[27] refined Schallamach's model by using a steady state stochastic model for debonding kinetics. Within this model, stretching of polymer chains occurs as a result of an external force, leading to the detachment of linking chains from the wall. The detached chain relaxes before reattaching to the interface, during which time it dissipates energy and relieves the tension accumulated during stretching. By considering the stochastic nature of detachment force, Chernyak and Leonov[27] derived the shear stress in dry sliding as given by eq 1

$$\sigma_t = \Sigma_o \frac{\int_0^\infty \varphi\left(\frac{r(t)}{\delta}\right) p(V,t)\, \mathrm{d}t}{V[\langle t\rangle_b + \langle t\rangle_f]} \tag{1}$$

In eq 1, $\Sigma_o$ is the areal density of the load bearing chains at zero velocity, $\varphi(r(t)/\delta)$ is the elastic energy stored in the polymer chain, $V$ is the sliding velocity, $\langle t\rangle_b$ is the mean lifetime of contact, $\langle t\rangle_f$ is the time the polymer chain spends in free state, and $p(V,t)$ is the transition probability of the polymer chain in going from the bonded to the relaxed state. The numerator of the Chernyak and Leonov equation (eq 1) is the work done in stretching the polymer chain to the breaking point, while the denominator represents the mean distance traveled by the chain. Multiplication of this stochastic force with the areal density of the linking chains gives rise to the expression for shear stress. Using a steady-state stochastic model of bond dissociation, Chernyak and Leonov showed that the mean lifetime of contact $\langle t\rangle_b$ and the transition probability depend on the sliding velocity as shown, respectively, in eqs 2 and 3.

$$\langle t_b\rangle = \tau_o\left\{1 - \exp\left(-\frac{V}{V_o}\right)\right\} \tag{2}$$

$$p(V,t) = \exp\left(-\frac{t}{\tau_o}\right)\left\{\delta(t - t_b) - \frac{\theta(t_b - t)}{\tau_o}\right\} \tag{3}$$

Here, $\delta(z)$ represents Dirac's delta function corresponding to the determinate process of forced break-off, and $\theta(z)$ is the Heaviside step function. With the above definitions

(23) Grosch, K. A. *Proc. R. Soc. London, Ser. A* **1963**, *274*, 21−39.
(24) Kontorova, T.; Frenkel, Y. I. *Zh. Eksp. Teor. Fiz.* **1938**, 8.
(25) Williams, M. L.; Landel, R. E.; Ferry, F. D. *J. Am. Chem. Soc.* **1955**, *77*, 3701−3707.

(26) Schallamach, A. *Wear* **1963**, *6*, 375−382.
(27) Chernyak, Y. B.; Leonov, A. I. *Wear* **1986**, *108*, 105−138.

of the bond survival time and the transition probability, eq 1 can be integrated for simple Gaussian polymer chains, the elastic energy of which is proportional to the square of the extension. Shear stress can then be expressed as follows:

$$\sigma = \sigma_a(m+1)\frac{u(1+s)\left(1 - \exp\left(\frac{-1}{u}\right) - \exp\left(\frac{-1}{u}\right)\right)}{m + 1 - \exp\left(\frac{-1}{u}\right)} \quad (4)$$

where $m$ is the fundamental ratio of the lifetimes of the polymer chain in the free and bound states at zero sliding velocity, $s$ is the ratio of the viscous retardation time over the lifetime at rest, and $u$ is the dimensionless velocity of sliding defined by eq 5

$$u = V\tau_o/\delta a \quad (5)$$

where $\tau_o$ is the lifetime of the bound state at rest and $\delta$ is the average distance between the polymer body and the wall. $\sigma_a$ is defined by eq 6.

$$\sigma_a = \frac{kT\Sigma_o\delta}{(1+m)R_F^2} \quad (6)$$

$R_F$ is the Flory radius of the polymer chain. Equation 4 predicts that the shear stress first increases with velocity in an S-shaped manner. After exhibiting a rather broad maximum, $\sigma$ usually decreases at very high sliding velocities.

Schallamach[26] and Chernyak and Leonov[27] developed their models envisioning purely adhesive sliding. However, Savkoor[28] as well as Ludema and Tabor[29] suggested that even seemingly adhesive sliding could never be purely adhesive. Savkoor[28] proposed a hybrid model, in which the interface consists of discrete patches of asperities of molecular dimensions in adhesive contact with the rubber surface. When a shear force is imposed, the patch stores elastic energy until it overcomes the adhesive energy, causing the propagation of a shear crack. According to Savkoor[28] as well as Ludema and Tabor,[29] sliding may proceed by an activated process, but the extent to which the two surfaces come into contact depends on modulus and sliding velocity. Hidden in more macroscopic terms, these approaches of Savkoor[28] and Ludema and Tabor[29] are similar to the model of Schallamach.[26]

In addition to the above molecular descriptions of rubber friction, there are other viewpoints, which can be important especially when the adhesion between the surfaces is dominated by specific short-range interactions, and/or when one of the materials is excessively compliant. In these cases, the surfaces do not easily slide relative to each other. Instead, the surfaces start peeling locally and detachment waves propagate throughout the entire area of contact starting from its advancing to the trailing edge. Schallamach[30] first discovered these waves at high sliding velocities. Roberts and Jackson[31] suggested that when such instabilities occur, the frictional stress between surfaces can be described in terms of the adhesion hysteresis ($\Delta W$), which is the difference between the energies involved in making and breaking interfacial contacts, and the wavelength ($\Lambda$) of the Schallamach instability, as $\sigma = \Delta W/\Lambda$. Recent theories of interfacial

friction of Rice,[32] Johnson[33] and Kim[34] invoke other dislocation models to describe the sliding of one surface against the other.

The above models, all of which offer plausible explanations for interfacial friction, have yet to be rigorously tested experimentally. The decoupling of the myriad factors contributing to interfacial friction requires not only a comprehensive experimental design but also the use of model elastomeric networks and well-characterized, model countersurfaces. The elastomeric networks would have to be chemically similar but differing in modulus, free of resins and fillers, and transparent for optical examination. Countersurfaces would have to be as smooth as possible and free of secondary interactions. The model interfaces would have to be robust enough to vary sliding velocity and temperature without compromising the ideality of the sliding materials.

Model studies of these types have recently been initiated by several authors. For example, Brown[35] and Casoli et al.[36] examined the pulling out of polymer chains from elastomeric networks and the associated friction. We[37] studied friction of poly(dimethylsiloxane) (PDMS) on some low energy surfaces as a function of molecular weight of the polymer and the sliding velocity. Although we noted that friction decreases with molecular weight, these studies were incomplete as the sliding speeds were rather small ($V < 4$ mm/s) and a limited molecular weight range of PDMS was used. In this paper, we extend these previous studies. The current studies were carried out with cross-linked elastomeric networks of PDMS sliding on two low energy surfaces: a methyl functional self-assembled monolayer (SAM) of hexadecylsiloxane and a thin film of polystyrene, both of which interact with PDMS via dispersion interactions. Using these simple model systems, we carried out the measurements of adhesion and friction to investigate how the latter depends on surface energy, temperature, velocity, and inter-cross-link molecular weight of the elastomer. Roughness was purposely avoided so that we could observe purely adhesive sliding as closely as possible.

## Experimental Section

**Materials.** The PDMS elastomers were cross-linked by platinum-catalyzed hydrosilation of vinyl end-capped siloxane[38] oligomers ($H_2C$=$CH(Si(CH_3)_2O)_nSi(CH_3)_2CH$=$CH_2$) with methylhydrogen siloxane cross-linker[39] (Syloff 7678: $(H_3C)_3O$-$(SiHCH_3O)_p(Si(CH_3)_2O)_qSi(CH_3)_3$). This reaction system with optimum combination of divinylsiloxane oligomer and the cross-linker yielded a highly cross-linked network with negligible byproducts. The molecular weights of the oligomers $M$ were 1.3, 1.8, 4.4, 8.9, 18.7, and 52.2 kg/mol. The oligomers were mixed thoroughly with Pt(IV) catalyst and maleate inhibitor before adding the cross-linker. The mass ratio of oligomer/catalyst/maleate was 97.4:1.9:0.7 for all molecular weights. The proportional amount of cross-linker added after thorough mixing varied with molecular weight as $23M^{-0.97}$, where $M$ is in kg/mol.

(32) Rice, J. R.; Ben-Zion, Y. *Proc. Natl. Acad. Sci.* **1996**, *93*, 3811.
(33) Johnson, K. L. *Langmuir* **1996**, *12* (19), 4510.
(34) Hurtado, A. J.; Kim, K.-S. *Mater. Res. Soc. Symp. Proc.* **1999**, *539*, 81−92.
(35) Brown, H. R. *Science* **1994**, *263*, 1411.
(36) Casoli, A.; Brendle, M.; Schultz, J.; Philippe, A.; Reiter, G. *Langmuir* **2001**, *17* (2), 388.
(37) Ghatak, A.; Vorvolakos, K.; She, H.; Malotky, D.; Chaudhury, M. K. *J. Phys. Chem. London, Sect. B* **2000**, *104*, 4018−4030.
(38) The PDMS oligomers were synthesized by ionic polymerization and supplied to us by Dow Corning Corporation. The number averaged molecular weights of these polymers were determined by gel-permeation chromatography and NMR. Oligomers having the following $M$ were used: 1.3, 1.85, 2.738, 4.44, 8.88, 18.72, 52.17 kg/mol.
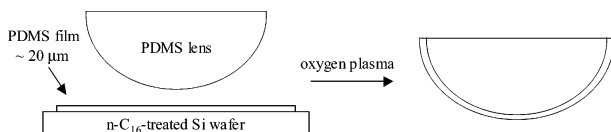(39) Syloff 7678 was characterized by Jim Tonge of Dow Corning and found to have $M_n$ and $M_w$ = 3.5 and 7.5 kg/mol, respectively. The SiH functionality makes up 70% of the molecule.

(28) Savkoor, A. R. *Wear* **1965**, *8*, 222−237.
(29) Ludema, K. C.; Tabor, D. *Wear* **1966**, *9*, 329−348.
(30) Schallamach, A. *Wear* **1971**, *17*, 301.
(31) Roberts, A. D.; Jackson, S. A. *Nature* **1975**, *257* (5522), 118−20.

**Figure 3.** The preparation of low-modulus samples for frictional testing. A thin (∼20 μm) film of the desired network is cast on a hydrophobic Si wafer. The air-exposed surface of the film and a higher-modulus lens are both plasma oxidized and welded together to form a composite lens which does not deform during friction measurements.

The resulting mesh sizes of the networks were estimated using the standard method of swelling in solvent (see for example Patel et al.,[40] who studied the properties of ideal PDMS networks). A sheet (1 mm thick) of each network was cured, from which small rectangular pieces having dimensions 2 cm × 2 cm were cut out. These were immersed in toluene (with which PDMS has a solvent interaction parameter $\chi$ of 0.465) overnight to ensure equilibrium swelling, after which their swollen dimensions were carefully measured. The equilibrium PDMS volume fraction $\phi$ in the present systems very closely resembled the results of Patel et al. In both cases, it may be approximated as $\phi = 0.7M^{-1/3}$, where $M$ is in kg/mol. The classic Flory−Rehner equation,[41,42] which assumes that the only connections between network chains are the chemical cross-links, fails in predicting the equilibrium volume fraction of PDMS. As described by Patel et al., the swollen dimensions of the present networks also corresponded to effective mesh sizes smaller than the oligomeric precursors. Patel et al. ascribe this phenomenon to the interspersion of oligomeric chains that are not relieved and, in fact, trapped by the formation of chemical cross-links. To calculate the effective mesh size, Patel et al. consider the experimentally measured equilibrium elastic modulus $E$ and invoke the affine model described by eq 7

$$M_e = \rho RT/E \qquad (7)$$

where $\rho$ is the density of the polymer.

We followed a procedure similar to that of Patel et al. To measure the equilibrium elastic modulus of each network, the method of contact mechanics as developed by Johnson, Kendall, and Roberts[43] (JKR) was used. Hemispherical lenses of each network were prepared by depositing small drops of the reaction mixture onto perfluorinated glass slides and cross-linking them at 120° for 50 min. These lenses were then brought in to and out of contact with the substrate of choice under controlled loads. The load-deformation data obtained from these experiments yielded not only the elastic moduli of the networks but also their adhesion energies with the countersurface.

For sliding friction measurements, the lenses were allowed to slide laterally on the substrates. It was however noticed that the low modulus ($M > 4.4$ kg/mol) hemispheres deform laterally, thus compromising the accuracy of the shear stress measurements. To avoid such complications, we transferred thin films of these high molecular weight PDMS onto more rigid lenses of PDMS ($M = 3.5$ kg/mol) according to a method described by Chaudhury.[44] Briefly, thin films (∼20 μm) of the high molecular weight PDMS elastomers were cast onto a silicon wafer, which was made nonadherend to the PDMS film by coating it with a monolayer of hexadecyltrichlorosilane. After both the PDMS film and lens were oxidized using plasma, they were pressed together for about 1 min, during which the plasma-oxidized polymers began to weld to each other. When the normal load was released, the PDMS lens peeled off the thin PDMS film from the silanized silicon wafer (Figure 3). These specially made lenses were not used immediately but were left in contact overnight to ensure secure welding between the thin film and the underlying lens.
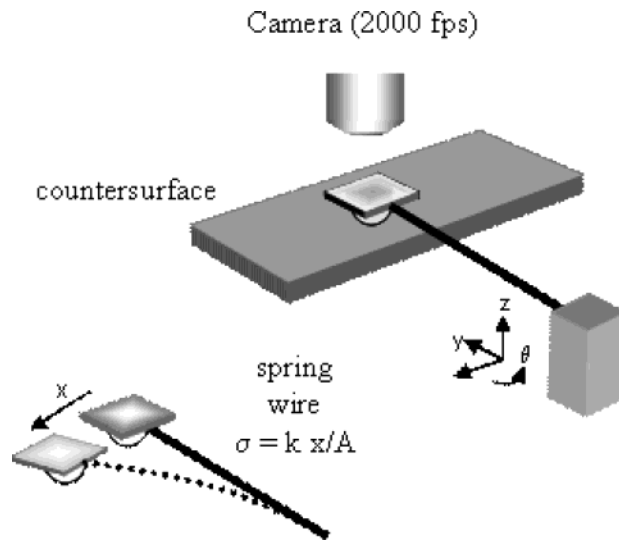
(40) Patel, S. K.; Malone, S.; Cohen, C.; Gillmor, J. R.; Colby, R. H. *Macromolecules* **1992**, *25* (20), 5241.
(41) Flory, P. J. *Principles of Polymer Chemistry*; Cornell University Press: Ithaca, NY, 1953.
(42) Flory, P. J.; Rehner, J. *J. Chem. Phys.* **1943**, *11*, 521.
(43) Johnson, K. L.; Kendall, K.; Roberts, A. D. *Proc. R. Soc. London* **1971**, *A324*, 301.
(44) Chaudhury, M. K. *J. Phys. Chem. B* **1999**, *103*, 6562.



**Figure 4.** The apparatus for frictional testing of elastomeric lenses. The lens is placed on the end of a calibrated spring, the deflection of which gives the frictional force. The frictional force, normalized by the contact area, yields the shear stress. Both the deflection and the contact area are viewed using a high-speed camera. Steady-state and velocity relaxation experiments are both performed using this setup.

Unreacted oligomers were extracted from all lenses with chloroform in a Soxhlet extractor for 12 h. They were then allowed to dry at room temperature for 1 week under a gentle vacuum (∼0.8 atm) before being used in any measurements.

Contact mechanics and friction measurements were performed against two low-energy surfaces: a self-assembled monolayer (SAM) of hexadecylsiloxane, and a thin film (∼100 μm) of polystyrene. The SAM was prepared by reacting a clean polished silicon wafer with the vapor of hexadecyltrichlorosilane according to a method previously published.[45] The surface energy of the resultant surface was ∼19 mJ/m², as estimated by the contact angle of hexadecane (45°), which exhibited negligible hysteresis, indicating lack of gross surface imperfections. The polystyrene film was prepared by casting a toluene solution of the polymer ($M = 1.5 \times 10^6$ g/mol) on a clean silicon wafer and allowing the solvent to evaporate slowly in a covered Petri dish at atmospheric pressure for 1 week.

**Contact Mechanics.** Following the well-known method of Johnson, Kendall, and Roberts,[43] a hemispherical lens was brought into contact with the substrate of interest at zero applied load. The lens was then loaded externally in a quasi-equilibrium manner up to a maximum load of 0.2 g. Subsequently, it was unloaded in the same manner. During each loading and unloading cycle, the contact area was viewed using a reflection microscope, while the load was recorded in an electrobalance interfaced to a personal computer. These load-deformation data were analyzed using the well-known JKR equation (8) in order to estimate the adhesion energy $W$ of the interface and the elastic modulus $E$ of the PDMS lenses

$$\frac{a^{3/2}}{R} = \frac{9}{16E}\frac{P}{a^{3/2}} + \frac{3}{4}\left(\frac{6\pi W}{E}\right)^{1/2} \qquad (8)$$

where $a$ is the contact radius, $R$ is the radius of curvature of the lens, and $P$ is the normal force.

**Measurement of Friction.** Frictional properties between the lenses and the countersurfaces were examined using two methods, both of which require use of the setup represented by Figure 4. In a manner reminiscent of Roth et al.,[14] velocity relaxation data were combined with steady-state data. The former data were obtained using a method described by Brown[35] and Chaudhury[2,46] to measure the friction at low sliding velocities.

(45) Chaudhury, M. K.; Whitesides, G. M. *Langmuir* **1991**, *7* (5), 1013.
(46) Chaudhury, M. K.; Owen, M. J. *Langmuir* **1993**, *9*, 29.

In this method, the lens was placed on one end of a calibrated spring, the other end of which was rigidly supported. After the lens was brought into contact with the substrate of interest, the latter was given a sudden displacement. The lens at first moved with the substrate but then relaxed back to its original position as the spring recovered its neutrality.

With the deflection of the spring monitored as a function of time, the force acting on the lens was determined as a function of sliding velocity. Division of this force by the contact area yielded the shear stress as a function of velocity. The velocity range thus achieved was from $10^{-7}$ to $10^{-3}$ m/s.

Measurements at higher velocities were obtained by sliding the substrate relative to the lens at uniform velocities while the lens rested on the edge of the calibrated spring. The velocity range of these steady-state measurements was from $10^{-4}$ to $10^{-1}$ m/s. Some measurements were taken at even lower velocities to ensure agreement with the relaxation data. Inertial forces were negligible in all these measurements. Up to a critical velocity, sliding was stable, beyond which the friction force exhibited stick–slip dynamics similar to that reported by Grosch.[23] When these instabilities occurred, friction force corresponding to the highest deflection of the spring was recorded, in accordance with Grosch's[23] procedure. This force, divided by the corresponding contact area (measured simultaneously by the camera), yielded the shear stress. The combination of the above two methods allowed us to measure the friction force in the range of $10^{-8}$–$10^{-1}$ m/s, comparable to the range of velocities employed by Reiter et al.[36] to study the effect of the pull-out of grafted PDMS chains from PDMS networks.

Shear stresses were invariant with respect to changes in normal load (5.5–120 mN for stable sliding, 24–50 mN for unstable sliding) and thus to the contact area. These findings are consistent with earlier findings of Homola et al.[47] and Chaudhury et al.[2,46] and indicate that the ratios of actual to nominal contact areas do not increase with increasing load, in contrast with the findings of Schallamach[17] and Bahadur,[48] and the predictions of Ludema and Tabor.[29]

Measurements at various temperatures were carried out by heating the substrate with an infrared lamp. The substrate temperature was carefully controlled by adjusting the distance of the lamp from the substrate and measured using a flat thermocouple (OMEGA SAJ-1) adhered to the substrate. The temperature range employed was 298–348 K. The substrates and the PDMS networks are all hydrophobic, but lower temperatures were not attempted as a precautionary measure, so as to avoid condensation effects. Higher temperatures were not attempted so as to avoid morphological changes in the Si wafers and/or an incipient glass transition in the PS thin film.

The PDMS networks were not reinforced with any resin or filler. As such, they were easier to abrade than commercial materials. The full range of molecular weight was allowed to slide against the SAM-covered wafer. However, the two lowest molecular weights ($M$ = 1.3 and 1.8 kg/mol) could not withstand the entire velocity range and abraded easily on the surface. Against the PS-covered wafer, only the networks with $M \geq 8.9$ kg/mol could withstand the sliding, even at low velocities.

**Roughness Measurement.** The root mean square roughnesses of the SAM (0.2 nm) and PS (0.5 nm) coated silicon wafers over an area of 1 $\mu$m$^2$ were measured by Olga Schaffer (Emulsion Polymer Institute, Lehigh University) using the method of atomic force microscopy (AFM).

The roughness values of the PDMS elastomers were generously provided by Yujie Sun and Gilbert Walker (University of Pittsburgh). The root mean square roughness values of all the elastomers were less than 0.5 nm except for the PDMS of $M$ 1.3 kg/mol, for which the roughness was estimated to be 1.0 nm. The roughness values of the PDMS elastomers are consistent with those found by Efimenko et al.[49] using both AFM and X-ray reflectivity measurements.

(47) Homola, A. M.; Israelachvili, J. N.; McGuiggan, P. M.; Gee, M. L. *Wear* **1991**, *136*, 65.
(48) Bahadur, S. *Wear* **1974**, *29*, 323–336.
(49) Efimenko, K.; Wallace, W.; Genzer, J. *J. Colloid Interface Sci.* **2002**, *254*, 306 and references therein.
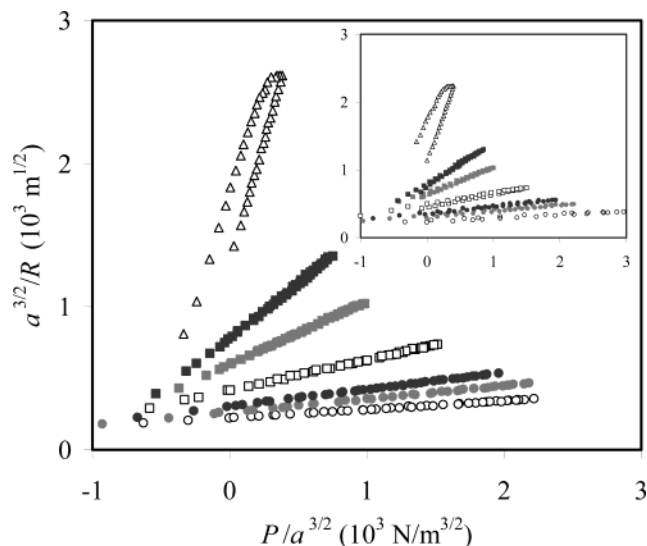


**Figure 5.** The contact area as a function of normal load allows calculation of the network modulus and the work of adhesion at each interface. As the slope of the line increases, the modulus decreases. The symbols open circle, gray circle, black circle, open box, gray box, black box, and open triangle represent networks with oligomeric precursors of 1.3, 1.8, 2.7, 4.4, 8.9, 18.7, and 52.1 kg/mol, respectively.

**Table 1. The Advancing Work of Adhesion for All Networks on the SAM- and PS-Covered Si Wafers[a]**

| $M$ (kg/mol) | $W_{\text{PDMS–SAM}}$ (mJ/m$^2$) | $W_{\text{PDMS–PS}}$ (mJ/m$^2$) |
|---|---|---|
| 1.3 | 42 | 53 |
| 1.9 | 41 | 55 |
| 2.7 | 44 | 56 |
| 4.4 | 42 | 53 |
| 8.9 | 42 | 52 |
| 18.7 | 42 | 44 |
| 52.1 | 27 | 26 |

[a] The strength of interaction is largely independent of molecular weight. The low values for $M$ = 52.1 kg/mol are attributed to viscoelasticity.

## Results

**Contact Mechanics.** The contact mechanics data are displayed in Figure 5, where $a^{3/2}/R$ is plotted against $P/a^{3/2}$. These plots, in conformity with eq 8, are straight lines, the slopes and intercepts of which yielded the values of $E$ and $W$, respectively. For PDMS of inter-cross-link molecular weights ($M$) of 1.3–18.7 kg/mol, the loading/unloading data do not exhibit any noticeable hysteresis either on the SAM- or on PS-coated Si wafers.
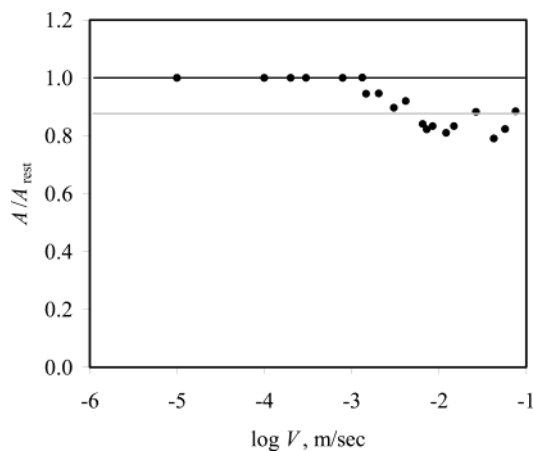
The works of adhesion on the SAM-coated wafer clustered around 41–42 mJ/m$^2$, being independent of the molecular weight (Table 1). For PDMS on the PS-coated wafer, these values were somewhat higher: 51–56 mJ/m$^2$. For the highest molecular weight PDMS (52.2 kg/mol), the loading cycle yielded values of $W$ as 27 and 26 mJ/m$^2$ on the SAM and PS, respectively, whereas the corresponding values were 55 and 68 mJ/m$^2$ during the unloading experiments. The finite hysteresis observed with this molecular weight resulted from slight viscoelastic deformation of the rubber, which is due to incomplete cross-linking of the network.[50]

As expected, the Young's modulus, as obtained from the above JKR analysis, is found to be inversely proportional to molecular weight (Figure 6).

**Contact Area during Sliding.** The combination of the transparency of PDMS, the reflectivity of the countersurfaces, and the use of the high-speed camera allowed direct examination of the contact area
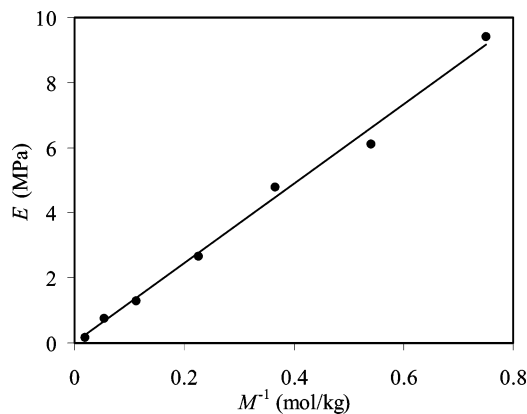
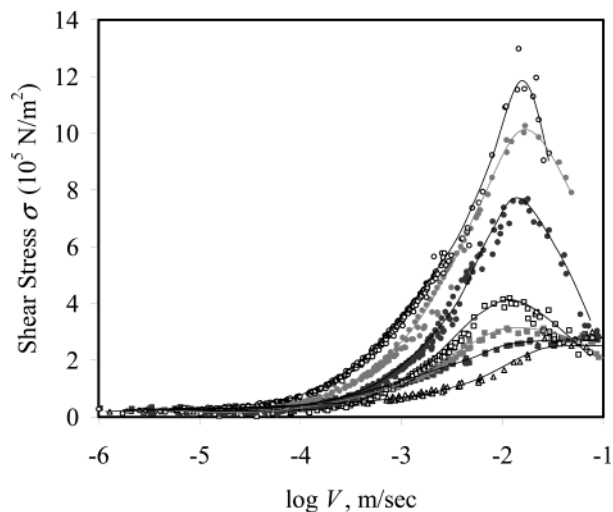**Figure 6.** Young's modulus $E$ is linear with inverse molecular weight $M^{-1}$.



**Figure 8.** Shear stress as a function of velocity between PDMS and the SAM-covered Si wafer. Open circle, gray circle, black circle, open box, gray box, black box, and open triangle represent networks with oligomeric precursors of 1.3, 1.8, 2.7, 4.4, 8.9, 18.7, and 52.1 kg/mol, respectively.



**Figure 7.** The ratio of sliding to resting contact area as a function of velocity for PDMS ($M = 2.7$ kg/mol, $R = 2.5$ mm, $E = 4.8$ MPa, $W = 42$ mJ/mol) against the SAM. As the sliding velocity increases, the contact area drops from the JKR prediction (black line) to the purely Hertzian prediction (gray line). The normal load $P$ averaged 48 mN (see eq 7).

as a function of velocity. Figure 7 shows that the contact area remains constant up to a sliding velocity of 1 mm/s. Only about 10% reduction of contact radius occurred close to the transition from smooth to stick–slip sliding, which appears to be due to the transition from JKR to Hertzian deformation resulting from the loss of adhesion as predicted by Savkoor and Briggs.[51]
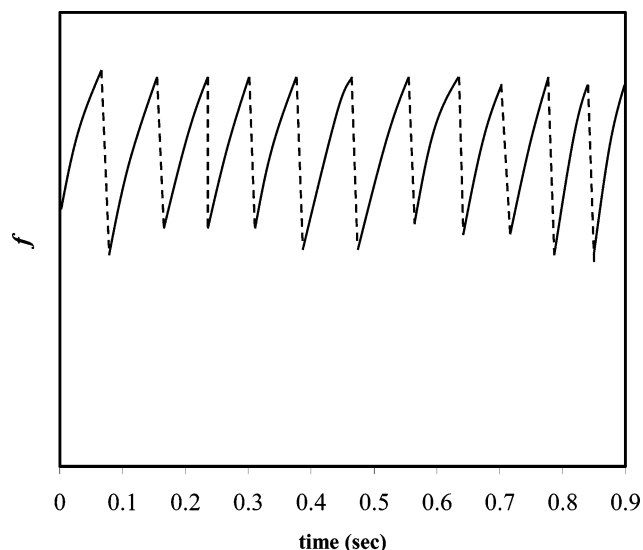
**Friction: System Dynamics.** The shear stress data of PDMS networks sliding on the SAM-coated wafer (Figure 8) show that $\sigma$ at first increases with velocity and then either levels out or decreases. Frictional force is stable when $d\sigma/dV \geq 0$. However, at the negative resistance branch ($d\sigma/dV < 0$) of the stress velocity cycle, frictional sliding is unstable and periodic (Figure 9) as was reported previously by Grosch.



**Figure 9.** Stick–slip sliding is characterized by a periodic friction force fluctuation. As the countersurface moves at a constant velocity, the elastomeric lens is simultaneously sliding and being deflected (solid curves). The actually sliding velocity increases up to the imposed velocity, at which point the interface slips (dashed lines). Here we have shown a typical force trace obtained with a PDMS of $M = 4.4$ kg/mol sliding at 2 cm/s on the SAM surface.

The spring deflection at the higher frictional stress achieved during these stick–slip limit cycles is the unstable focus point.[52] At a given imposed velocity, friction force reaches a maximum value when the lens slips by a certain distance before it is captured by the substrate and brought back to the point of maximum stress to repeat the process. Such sliding instability occurs when the spring constant is less than a critical value given by eq 9

$$k < k_c = -\frac{V}{d_0} A \frac{d\sigma}{dV} \qquad (9)$$

where $V$ is the imposed velocity, $A$ is the contact area, and $d_0$ is known as the memory length, which is typically on

---

(50) These advancing and receding works of adhesion are essentially the strain energy release rates ($G$). In the advancing mode, the energy to close the crack comes from the thermodynamics work of adhesion ($W$), which is equal to the strain energy release rate ($G$) plus the energy loss ($\Phi$) due to viscoelastic deformation of the polymer. Thus the measured strain energy release rate is less than the work of adhesion, i.e., $G = W - \Phi$. Conversely, when the crack is opening, the viscous dissipation *adds* to the strain energy release rate, as the material must be deformed before it detaches from the surface, thus increasing the receding work of adhesion ($G = W + \Phi$). See the following reference for more details: Johnson, K. L. In *Microstructure and Microtribology of Polymer Surfaces*; ACS Symposium Series 741; American Chemical Society: Washington, DC, 2000; pp 24−41.
(51) Savkoor, A. R.; Briggs, G. A. D. *Proc. R. Soc. London, Ser. A* **1977**, *356*, 103.

(52) Ronsin, O.; Coeuyrehourcq, K. L. *Proc. R. Soc. London, Ser. A* **2001**, *457*, 1277.

the order of the distance between the surface asperities. At the onset of instability, $d_o/V$ is on the order of the relaxation time ($10^{-7}$ s) of the polymer and $A(d\sigma/dV)$ is on the order of $0.1-1.0$ N s/m. Substitution of these values in eq 8 yields the magnitude of the spring constant ($\sim 10^7$ N/m) that would be required to avoid sliding instability. The spring constants used in our experiment are on the order of $10^2$ N/m, which is much smaller than $k_c$. Hence, sliding instability always occurs in our experiments, even when $d\sigma/dV$ is slightly negative. When such instabilities occur, we record the maximum shear stress just before the lens slips.

**Friction: Effects of Molecular Weight, Velocity, and Temperature.** There are about four important features of the kinetic friction observed in our experiments:

1. The friction decreases with the molecular weight.

2. The friction increases with velocity, reaches a maximum, and then either decreases or plateaus out.

3. The peak velocity is nearly independent of the molecular weight.

4. The friction peak broadens with molecular weight. It becomes independent of velocity when the molecular weight of PDMS reaches 18.7 kg/mol.

As is the current situation, there is no complete theory of kinetic friction that can account for all the observations summarized above in precise quantitative terms. The observations are, however, qualitatively consistent with the stochastic theory of rubber friction, as discussed below.

First, let us consider the inverse relationship between rubber friction and molecular weight, which has already been observed with melts[53,54] and grafted polymer chains.[2,37] To understand this observation, let us consider Ludema and Tabor's[29] suggested relationship between the shear stress $\sigma$ and the areal density ($\Sigma_o$) of the contact points as $\sigma = \Sigma_o f_o$, where $f_o$ is the force needed to detach a single polymer chain during sliding. This is similar to the prefactor in the Chernyak−Leonov equation (4) corresponding to the shear stress in the high velocity limit, i.e., where the detachment of the polymer chain from the surface is not controlled by stochastic processes. Within the simple model developed by Chernyak and Leonov,[27] the areal density of the load-bearing chains is $1/Na^2$, $N$ being the number of statistical segments, each of size $a$. One thus obtains that the shear stress is proportional to the shear modulus as $\sigma = Gf_o a/kT$. The Chernyak−Leonov[27] model is, however, not applicable to a real elastomer, where the areal density of polymer chains scales as $N^{-1/2}$. One thus anticipates a relationship between shear stress and shear modulus as $\sigma \sim G^{1/2}$. Experimentally, however, a power law exponent close to 3/4 has been observed (Figure 10). While Grosch[23] did not systematically study the effect of modulus on friction, he noted that the shear stress he obtained is considerably smaller than that expected of two surfaces in true molecular contact. To account for the discrepancy, Grosch estimated the actual area of contact to be approximately 10% of the apparent contact area during sliding.[23] In our case, the AFM studies indicate that both the PDMS and the countersurfaces are smooth to nanometer length scales. Hence, gross mismatch of interfacial contact is not expected based on roughness considerations. However, it is plausible that spontaneous roughening of the interface occurs as a result of elastic instability, which ensues from the competition between van der Waals and elastic forces within the first layer of stretched PDMS chains in contact
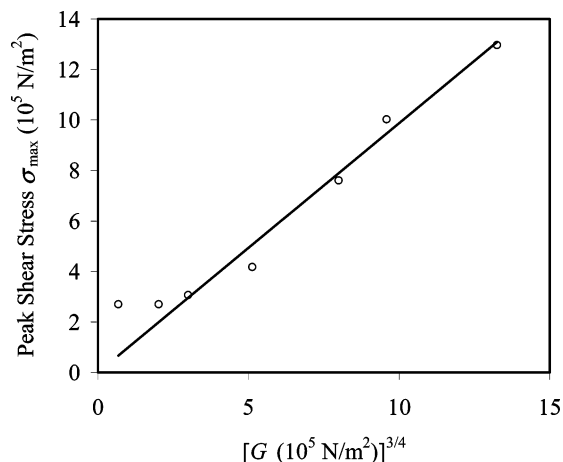


**Figure 10.** Peak shear stress $\sigma_{max}$ between PDMS and the SAM-covered Si wafer is proportional to $G^{3/4}$.

with the surface. If we consider that the dominant wavelength of such roughening scales with the thickness ($\delta$) of the first layer of the polymer chain, then the density of the load-bearing sites should scale as $1/\delta^2$ (or $1/Na^2$). If one polymer chain remains active in each of the load-supporting junctions, one essentially recovers the result: $\sigma \sim G$. Shear stress should decrease with the molecular weight because the number of load-bearing polymer chains decreases with molecular weight. However, when the molecular weight reaches rather high values ($M \geq 18.7$ kg/mol), $\sigma_{max}$ becomes nearly independent of molecular weight. At high molecular weights, the above simple analysis becomes less effective, due to complications arising from the entanglement effects.

The dependence of shear stress on molecular weight also addresses a long-standing question on the relationship between friction and energy losses due to bulk viscoelastic deformation. Up to now, interfacial friction force has been largely attributed to bulk dissipation,[21,22,62] which arises due to cyclic deformation and relaxation cycles of the rubber moving over rough asperities. We purposely chose molecularly smooth surfaces so as to avoid such bulk dissipation. Even if we consider the effect of bulk dissipation in frictional loss, the observed trend is quite opposite to the predictions based on their bulk rheological data. Gordon et al.[55] reported the storage and loss moduli of several cross-linked PDMS networks similar to the present ones, which show that the viscoelastic loss measured in terms of the phase angle ($\delta$) increases with molecular weight (typically at a low frequency ($a_T\omega \sim 10$ Hz), the phase angle varies with molecular weight as log($\tan \delta$) $\sim 0.1M$, where $M$ is in kg/mol). If friction is caused by bulk dissipation, shear stress should increase with molecular weight. We, in fact, observe just the opposite behavior: shear stress decreasing with molecular weight, thus clearly pointing out that the frictional dissipation for the PDMS elastomers is not due to the bulk viscoelastic deformation.

It is noteworthy, as shown in Figure 8, that the velocity at which stick−slip transitions occur is nearly independent of the molecular weight of the polymer for all molecular weights of PDMS (except for $M = 52.2$ kg/mol). According to Grosch, this transition should occur at a velocity $V_o$ given by the ratio of a molecular length scale ($\lambda \sim 7$ nm) and the relaxation time of the polymer chain. This critical velocity, according to Chernyak and Leonov, appears at

(53) Inn, Y.; Wang, S.-Q. *Phys. Rev. Lett.* **1996**, *76* (3), 467−470.

(54) Hirz, S.; Subbotin, A.; Frank, C.; Hadziioannou, G. *Macromolecules* **1996**, *29*, 3970−3974.

(55) Gordon, G. V.; Owen, M. J.; Owens, M. S.; Perz, S. V.; Stasser, J. L.; Tonge, J. S. *Proc. Annu. Meet. Adhes. Soc.* **1999**, 424.
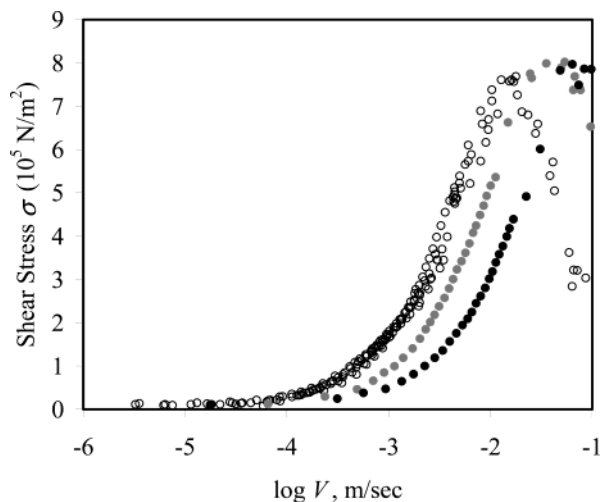
**Figure 11.** Shear stress as a function of velocity and temperature between PDMS and the SAM-covered Si wafer for $M$ = 2.7 kg/mol. Open circle, gray circle, and black circle represent data at 298, 318, and 348 K, respectively.



**Figure 12.** The temperature-dependent shear stress data shifted to room temperature using an Arrhenius shift factor. The activation energy of sliding between PDMS and the SAM is thus estimated to be 25 kJ/mol. Open circle, gray circle, and black circle represent data at 298, 318, and 348 K, respectively.

$V_o = \delta \cot \chi / \tau_o$. As $\delta \sim N^{1/2}a$ and $\cot \chi \sim f_o\delta/kT$, $V_o \sim f_oNa^2/kT\tau_o$. Here the relaxation time of the polymer chain $\tau_o$ is related to the segmental level relaxation time $\tau$ as $\tau_o = \tau N^\beta$, $\beta$ being an exponent the value of which depends on the mode of relaxation of the polymer chain. Chernyak and Leonov proposed the value of $\beta$ to be 3/2 (an unlikely scenario in dense state), which results in the molecular velocity $V_o$ decreasing with $N$ following a 1/2 power law. Experimental observation is that $V_o$ is nearly independent of the molecular weight of the polymer, suggesting a value of $\beta$ close to unity. Thus, $V_o$ appears to be the segmental level velocity of the polymer chain on the surface as conjectured by Grosch,[23] who estimated this relaxation time from the frequency ($\omega$) at which the loss modulus of the polymer exhibits a maximum. Unfortunately, such a comparison is not possible for PDMS, as its segmental relaxation frequency is so high that it has not been possible to measure it by rheological spectroscopy. On the basis of the fact that the segmental length of PDMS is 0.6 nm, and that the friction peaks appear at a sliding velocity of 1 cm/s, the relaxation time of PDMS segments in contact with the methyl SAM coated surface is estimated to be $\sim 10^{-7}$ s. This time is considerably larger than the viscous relaxation time ($10^{-11}$ s) of dimethylsiloxane monomer,[56] suggesting that the mobility of the polymer chain is severely modified by its interaction with the surface. Further support to this conjecture is given below.

**Friction as an Activated Rate Process.** Shear stress of PDMS depends on temperature, as shown in Figure 11 for PDMS sliding on the SAM surface. If rubber friction is a thermally activated rate process, then it should be possible to shift the shear stress data obtained at different temperatures to room temperature by multiplying the sliding velocities with a suitable shift factor. As the glass transition temperature ($T_g \sim -130$ °C) of PDMS is far lower than any of the testing temperatures, an Arrhenius shift factor $a_T$ (eq 10) is adequate for the above purpose.

$$\log a_T = \frac{E_a}{2.3R}\left[\frac{1}{298} - \frac{1}{T}\right] \qquad (10)$$

From the shift factor used to unify the temperature-dependent data (see Figure 12), the activation energy ($E_a$) of sliding of PDMS on the SAM-covered wafer was found
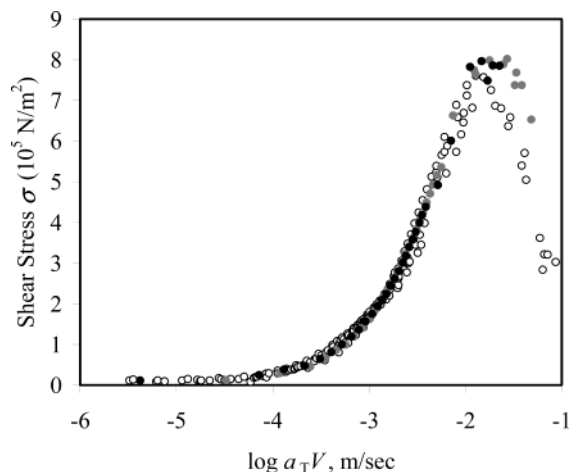
to be 25 kJ/mol. This activation energy is also found to be independent of molecular weight but is five to six times larger than the typical depth of a van der Waals potential well.

Stein et al.[57] have studied the dynamics of PDMS chains in the melt state by measuring the fluorescent decay of a probe chromophore. They noted that the thermally activated local dynamics follow an exponential behavior with activation energies in the range of 20−27 kJ/mol, which are considerably higher than the activation energy (13−16 kJ/mol) of viscous flow but close to that observed in our dynamic friction studies.

On the basis of the above values of activation energy (25 kJ/mol) and relaxation time ($10^{-7}$ s), it is tempting to estimate the pre-exponential factor $\tau^*$ of the Arrhenius equation $\tau = \tau^* \exp(E_a/RT)$. $\tau^*$ is estimated to be on the order of $10^{-12}$ s, which is very close to the value ($h/kT$) predicted by Eyring.[20] This is somewhat a surprising result, as the pre-exponential time scale for the diffusion of polymeric segments on surfaces[61] is usually a few orders of magnitude higher than the elementary time scale in Eyring's kinetics.

**Peak Broadening with Molecular Weight.** An important observation of these friction data is that the peak at which maximum friction occurs broadens as the molecular weight increases. To understand this effect, we recall the models of Schallamach[26] and Chernyak and Leonov,[27] which suggest two types of processes occurring at the interface during frictional sliding: the debonding force increasing with velocity, while the number of the load-bearing polymer chains ($\Sigma$) decreases with velocity.

The detachment force, in general, is controlled by the stochastic process, until very high velocities. The areal density of the load-bearing sites however decreases with velocity, as the time of detachment of the polymer chain decreases and thus approaches its free relaxation time. At any given velocity, $\Sigma(t)$ can be expressed in terms of the bonded and relaxed time of the polymer as follows

$$\Sigma = \Sigma_o \frac{\langle t \rangle_b}{\langle t \rangle_b + \langle t \rangle_f} \qquad (11)$$

where $\langle t \rangle_b$ is the time of contact between the polymer chain

(56) Appel, M.; Fleischer, G. *Macromolecules* **1993**, *26*, 5520.

(57) Stein, A. D.; Hoffman, D. A.; Marcus, A. H.; Leezenberg, P. B.; Frank, C. W.; Fayer, M. D. *J. Phys. Chem.* **1992**, *96*, 5255.
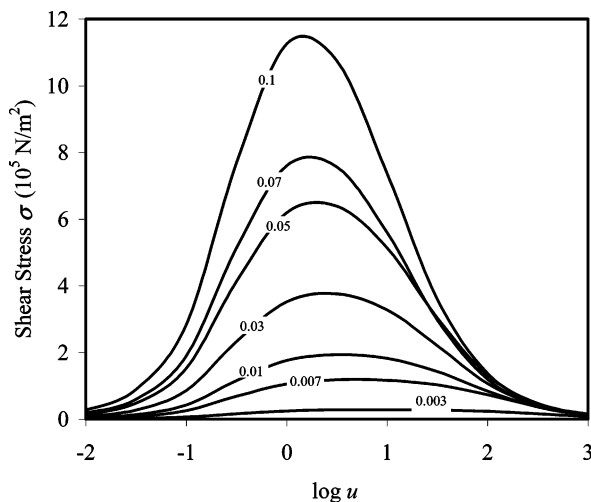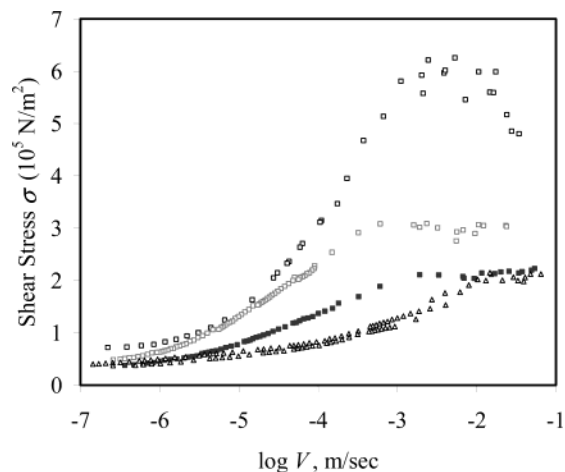
**Figure 13.** Shear stress as a function of velocity as predicted by the Chernyak−Leonov model for adhesive friction. The value *m* is the ratio of the lifetimes of the polymer chain in the free and bound state.

and the substrate and $\langle t \rangle_f$ is the relaxation time of the polymer chain in the unbonded state. Chernyak and Leonov[27] argued that all the segments of a polymer chain have to be activated for it to desorb from a surface. While a catastrophic desorption of the polymer chain may not represent the reality, the alternative possibility that desorption is a sequential process akin to peeling is equally consistent with the lifetime of contact being proportional to molecular weight. The lifetime of contact, as shown in eq 2, however, decreases with velocity. For higher molecular weight polymers, a larger velocity must be reached before the chain desorbs from the surface. It is thus expected that the peak corresponding to the stick−slip transition should broaden with molecular weight.

On the basis of the above discussions, we note that the Chernyak−Leonov[27] model, as embodied by eq 4, takes into account most of the results of PDMS rubber sliding on the SAM-coated silicon wafer. To examine the full prediction of this model, we simulated the frictional shear stresses of a rubbery network on a surface using eq 4 under two simplified assumptions. The first is that the term $(m + 1)\sigma_a \cot \chi$ is replaced by the shear modulus *G*. The second assumption is that the nondimensional velocity *u* is independent of the molecular weight. The parameter *m*, which is the ratio of the relaxation time of the polymer segment in the detached state to that in the adsorbed state, is varied from 0.1 to 0.003 in order to observe the general effect of molecular weight on peak breadth. These simulations, as summarized in Figure 13, show that the peak width indeed increases with molecular weight of the polymer. For very small values of *m* (i.e., at very high molecular weights), a plateau is observed. Experimentally, however, we are restricted to the plateau region of the peak.

**Frictional Behavior of PDMS on Polystyrene.** As shown in Figure 14, the general pattern of friction of PDMS on PS (i.e., its dependence on sliding speed and molecular weight) is similar to that on the SAM. The friction decreases with molecular weight. It increases with the sliding speed, then reaches a critical velocity beyond which it either decreases or exhibits a plateau. The velocity at which the friction reaches a maximum or a plateau is, at most, an order of magnitude lower than that observed with SAM. What is significantly different between the two surfaces is their behavior in the range of low velocity,



**Figure 14.** Shear stress as a function of velocity between PDMS ($M \geq 8.9$ kg/mol) and the PS-covered Si wafer. The onset velocity of stick-slip sliding ($\sim10^{-3}$ m/s) is an order of magnitude lower than on the SAM-covered wafer. Open box, gray box, black box, and open triangle represent networks with oligomeric precursors of 4.4, 8.8, 18.7, and 52.1 kg/mol, respectively. Networks of smaller precursors abraded against polystyrene, not allowing shear stress to be measured across the entire velocity range.
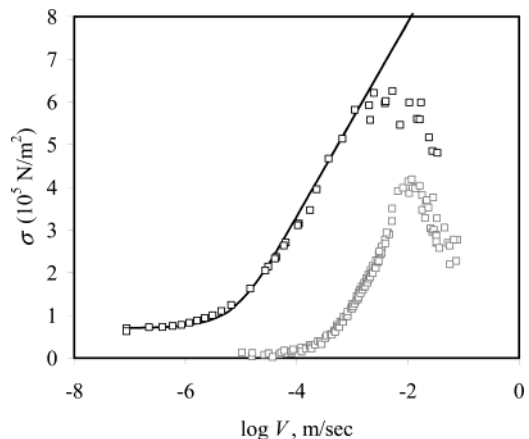


**Figure 15.** A comparison of the shear stress exhibited by PDMS ($M = 4.4$ kg/mol) on PS (black box) and the SAM (gray box). The black trendline is the prediction of eq 10. The maximum friction on each surface is attained at only slightly different velocities, but the low-velocity behavior differs drastically.

where polystyrene exhibits a much larger tail than SAM (Figure 15).

To understand whether this difference in chain mobility is reflected in the activation energy of kinetic friction, frictional stresses were measured at different temperatures. These kinetic friction data, when shifted to room temperature using the Arrhenius transform as done with the SAM data, yield an activation energy of $\sim27$ kJ/mol, which is nearly same as that observed on a SAM. Thus the difference of friction on the two surfaces could not be explained on the basis of their energetics. Differences of surface roughness cannot clearly explain this difference either, as the countersurfaces used for these experiments are smooth down to nanometer length scales (0.2 nm on a SAM and 0.5 nm on PS). The slight difference in surface roughness, should they play a role in the sense that energy dissipation increases in the bulk, ought to shift[23] the friction peak on the PS to a slightly higher velocity. Thus the low velocity frictional behavior on the two surfaces must originate from other mechanistic effects not considered in the present theories so far. One such possibility would be to consider the coupled dynamics of the poly-

styrene and PDMS chains at the interface. The possibility of chain interdigitation is not intuitive considering the fact that polystyrene is glassy and PDMS is rubbery. However, several recent studies have raised the possibility that the surface of polystyrene could be in the more relaxed state on the surface than in the bulk at room temperature.[58,59] In our experiments, there is no clear evidence of interdigitation between PDMS and PS as no remarkable adhesion hysteresis between the two is evident in the contact mechanics experiments (Figure 5). It can however be argued that an adhesion hysteresis as low as 1 mJ/m², which is beyond the limit of the measurement accuracy, could translate to an interfacial shear stress of 200 kPa by assuming the characteristic distance of segmental hopping to be ~5 nm.[60] Thus, while the possibility of a very small degree of interdigitation between PDMS and PS cannot be altogether eliminated, it is also plausible that the molecular tortuousity of the PS surface could play an important role, especially by affecting the pre-exponential time of the surface diffusion. It is plausible then that the kinetic friction of PDMS on polystyrene comprises two phenomena. In the low velocity limit, the effects of molecular rugosity and/or surface diffusion could contribute to friction, whereas at high velocities, friction is controlled by stochastic processes of adsorption and desorption as envisaged by Schallamach[26] and Chernyak and Leonov.[27] The velocity ($10^{-3}$ m/s) at which the maximum friction occurs yields a characteristic time scale of the process as $\tau \sim 10^{-6}$ s, which is not very different from that observed with the PDMS on SAM. However, the low velocity behavior of PDMS on PS should be treated differently. Assuming that the low velocity frictional behavior is controlled by a surface diffusion, the kinetic friction could follow an equation of the type

$$\sigma = \sigma_0 \sinh^{-1}(V/V^*) \qquad (12)$$

where $\sigma_o$ is a constant and $V^*$ is a characteristic velocity.

Equation 12 fits the low velocity ($V \leq 10^{-3}$ m/s) data rather well for all the molecular weights of PDMS, from which the estimate of the characteristic velocity $V^*$ is averaged to be ~6 $\mu$m/s. Figure 16 compares the shear stress for $M = 4.4$ kg/mol on the SAM and the PS and shows how well eq 12 fits the low velocity behavior on the latter surface. With this value of $V^*$ and the characteristic length as the segmental length (0.6 nm) of PDMS, the characteristic time scale of the frictional process is estimated to be ~$10^{-4}$ s, which is 2 orders of magnitude larger than that (~$10^{-6}$ s) corresponding to maximum shear stress. The pre-exponential factors ($10^{-9}$ and $10^{-11}$, respectively) of these two latter processes are also significant. The latter time scale corresponds to a classical Arrhenius process, whereas the former is typical of diffusional processes, the range observed in polymer chain folding kinetics.[61]

## Summary

This study reveals the richness and complexity of rubber friction on interfaces dominated by van der Waals interactions. The dependence of rubber friction on molecular weight, temperature, normal load, sliding velocity, and the nature of the countersurface can be understood qualitatively using the original ideas of Grosch,[23] Schallamach,[26] and Chernyak and Leonov.[27] A main factor contributing to rubber friction is the molecular weight of the polymer, which determines the areal density of the load-bearing junctions.

The overall behavior of rubber friction is consistent with the stochastic kinetics of adsorption and desorption of polymeric chains to surfaces for which two time scales are relevant: the relaxation time in the free state, and the time the polymeric chain spends in the adsorbed state. The latter time increases with the molecular weight of the polymer, leading to the broadening of the friction peak. Although these frictional characteristics can be described by the theory of absolute reaction rates, they are largely independent of the work of adhesion. Interestingly, what varies significantly among different surfaces is not so much the activation energy, but the pre-exponential factor in the Arrhenius equation, which indicates the contributions of other mechanistic processes not considered in the simple stochastic models of Schallamach and that of Chernyak and Leonov.

(58) Meyers, G. F.; Dekoven, B. M.; Seitz, J. T. *Langmuir* **1992**, *8*, 2230 (and references therein.)

(59) Wallace, W. E.; Fischer, D. A.; Efimenko, K.; Wu, W.-L.; Genzer, J. *Macromolecules* **2001**, *34* 15, 5081.

(60) Yoshizawa, H.; Chen, Y. L.; Israelachvili, J. *J. Phys. Chem.* **1993**, *97* (16), 4128.

(61) Smith, J.; Cusack, S.; Tidor, B.; Karplus, M. *J. Chem. Phys.* **1990**, *93* (5), 2974.

(62) Persson, B. N. G. *Sliding Friction: Physical Properties and Applications*, 2nd ed.; Springer: Heidelberg, 2000.